Hall-mobility measurements at elevated temperatures and pressures

Uzi Even, Menahem Levine, Jacob Magen, and Joshua Jortner

Department of Chemistry, Tel-Aviv University, Tel-Aviv, Israel
(Received 2 June 1972)

We describe a system for the measurement of the Hall mobility in expanded liquid metals and in dense metallic vapors at elevated temperatures (30–1600 °C) and pressures (1–2000 atm). Performances of the experimental setup are presented for mercury up to its critical point.

I. INTRODUCTION

Measurements of the Hall mobility[1,2] in expanded liquid metals and in dense metallic vapors[3,4] can yield valuable information concerning the transport properties and the nature of the metal-nonmetal transition in a disordered system. The metal-nonmetal transition in a one-component system can be induced by varying the density of the dense metallic fluid.[3,4] Such density changes can be achieved relatively easily near the thermodynamic critical point (see Table I). The high temperatures (up to 2000 °C) and pressures (up to 2000 atm) involved in Hall-effect measurements for mercury and for some alkali metals in the vicinity of their critical point introduce several serious complications in the design of the experimental system. The main experimental problems involved in such measurements are (a) compatibility of materials for higher-temperature work; (b) chemical stability of materials against attack by metallic fluids at elevated temperatures and pressures; (c) introducing a magnetic field into a high-pressure vessel; (d) wide impedance range of the Hall generator sample near the metal-nonmetal transition; (e) detection of low voltages (10^{-9} V) in the presence of large interference signals and thermal noise; (f) elimination of large galvanomagnetic and thermomagnetic[1,2] voltages.

Some of these experimental difficulties [points (e) and (f)] can be overcome by the use of the double ac method[1,2] for Hall-effect measurements. As the double ac method has been described in detail[1,2] we shall not repeat here the underlying physical principles. This method can eliminate the parasitic galvanomagnetic and thermomagnetic[1,2] voltages, reject interference signals and thermal noise, and make possible the detection of low-level (10^{-9} V) signals.

We have constructed a high-temperature–high-pressure system for the measurements of the Hall effect and of the electrical conductivity[3,4] of subcritical expanded liquid mercury and of supercritical dense mercury vapor. Modifications of the measurement cell and of the furnace (see Sec. II) will enable the use of this system for studies of the Hall mobility in other subcritical and supercritical metal fluids. In what follows, the system components will be described.

II. MEASUREMENT CELL AND FURNACE

A rectangular liquid-metal sample (i.e., mercury) is contained in a 99.7% recrystallized alumina cell (Fig. 1) consisting a two parts: (a) a long (15 cm) six-bore cylinder (20-mm o.d.); (b) an alumina cap with a rectangular (0.5 mm) depression. The two parts are sealed together by a glass fritt characterized by a high softening point (Owen, Illinois 01328). Sealing is achieved by heating the two parts with the glass fritt, in an argon-filled furnace at 1300 °C. The glass melts and diffuses into the alumina and the joint so formed retains its sealing and strength even above the initial softening point of the glass. Electrodes for electrical measurements consist of molybdenum wires (1-mm o.d.). These are sealed by the same process to the upper end of the six base tube via a niobium bypass (see details in Fig. 1). Niobium was chosen for the seal because it matches the thermal expansion of alumina and is readily wetted by the sealing glass. Molybdenum was chosen for the electrode wire for the following reasons: (a) it is not attacked by mercury at elevated temperatures (1600 °C); (b) it makes a perfect Ohmic contact with mercury (in contrast to niobium or tantalum which are covered by a thin oxide layer, making a non-Ohmic contact). A niobium spiral pipe (10 cm long), which was also sealed at the upper end of the cell (Fig. 1), was used for filling the cell, and for preventing diffusion of high-pressure argon (used to balance the mercury vapor pressure) to the measurement area. The helium-leak-tested cell retained its vacuum tightness after several hours at 1500 °C. The dimensions of the metal sample are 15×13 ×0.5 mm. The ceramic parts were machined by Adolf Meller Co.

The furnace was prepared by noninductive winding of a molybdenum wire on an alumina substrate. Thermal in-

TABLE I. Thermodynamic critical points of some metals

Metal	Hg[a-c]	Cs[d]	Rb[e]	K[e,f]	Na[e]	Pb[g]	Sn[g]
Critical temperature (K)	1763	2023	2057	2198	2573	5400	8720
Critical pressure (atm)	1510	110	157	155	350	850	2100

[a]E. Franck and F. Hensel, Phys. Rev. **147**, 109 (1966).
[b]See Ref. 4.
[c]F. Birch, Phys. Rev. **41**, 641 (1932).
[d]H. Renkert, F. Hensel, and E.U. Franck, Ber. Bunsenges. Phys. Chem. **75**, 507 (1971).
[e]I. G. Dillon, P.A. Nelson, and B.D. Swanson, J. Chem. Phys. **44**, 4229 (1966).
[f]W.F. Freyland and F. Hensel, Ber. Bunsenges. Phys. Chem. **76**, 347 (1972).
[g]A.V. Grosse and J. Ivory, Nucl. Chem. **22**, 23 (1961). The critical data for Pb and Sn are estimated values only.

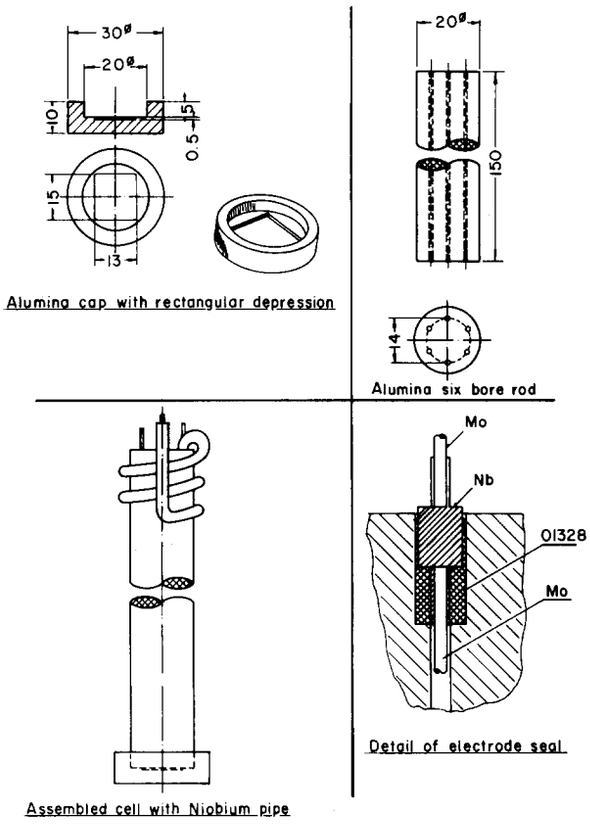

FIG. 1. Alumina cell (dimension in mm).

sulation was achieved by compressed zirconia powder.

The temperature was measured by a W/W 25% Re thermocouple and controlled by a three-term controller (proportional, integral, and differential). The controller (D. H. S. by Eurotherm, England) fed a 3-kW saturable reactor. This mode of control eliminated high-frequency interference introduced by a silicon-controlled rectifier or by relays. Temperatures in the range 30—1500 °C were measured to an accuracy of ± 6 °C and stabilized to ± 0. 2 °C.

III. HIGH-PRESSURE SYSTEM

High pressure is required to balance the vapor pressure of mercury and to control the density near the critical point ($P_e = 1510$ atm; $T_c = 1490$ °C, see Table I). Since we are not aware of any material which could withstand the high pressure at this high temperature, an internally heated pressure vessel, its walls maintained at room temperature, was designed and constructed (American Instruments). The internal volume (25 liter) of this pressure vessel (Fig. 2) is sufficiently large to contain the measurement cell, the furnace with its thermal insulation, the magnet coil, and the magnetic shield. The large volume and the high pressures involved imposed some safety problems. The pressure vessel is covered by a heavy gauge steel base, surrounded by protecting walls, and is remote controlled.

Electrical feedthroughs in the cap of the pressure vessel are of the coaxial type to reduce pickups and intermodulation distortion of signals by the high nonlinearities in the steel walls of the pressure vessel. High-purity argon (100 ppm total impurity content) was introduced into the vessel (after evacuation by a rotary vacuum pump) via a two-stage diaphragm compressor (American Instruments Co.). Pressure (10—2000 atm) was measured by a Bourdon-type gauge (Heise Bourdon Tube Co.) to within ± 2 atm.

IV. MAGNETIC FIELD

In view of the limited volume of the pressure vessel, only a magnetic field of moderate strength (100 G) could be maintained at the hot sample. The magnet had to be located inside the high-pressure vessel, as the alternating magnetic field is strongly absorbed by the steel walls of the pressure vessel. The magnetic field was generated by ten turns of an air-core coil. The coil was constructed from a copper-plated high-pressure stainless-steel pipe. The dimensions of the magnet were diameter 200 mm, length 300 mm, and coil wall thickness 3 mm. The large current (~300 A) flowing through the coil dissipated about 3 kW, requiring water cooling of the high-pressure pipe. The alternating magnetic field (at 1600 Hz) has to be shielded from the pressure vessel to eliminate induced eddy currents (which will attenuate the magnetic field considerably). Shielding was achieved by a cylinder surrounding the coil. This cylin-

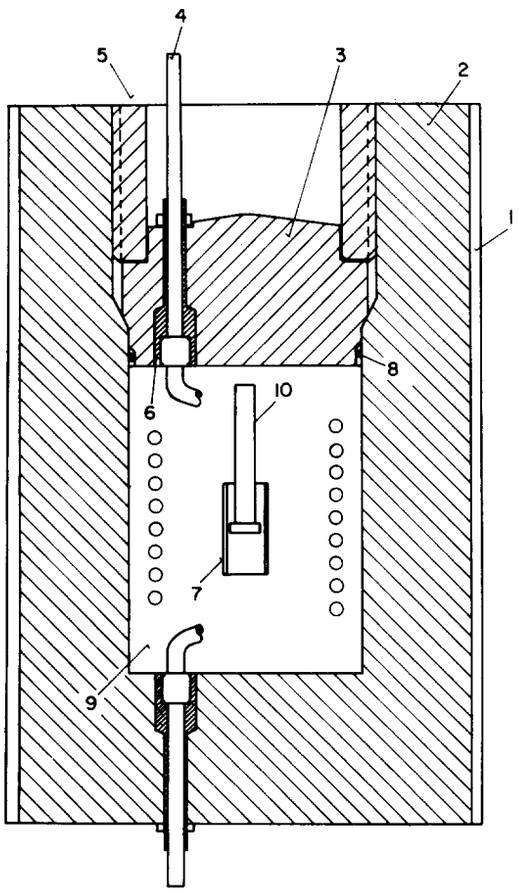

FIG. 2. General description of the pressure vessel and its internal parts. 1: Water jacket. 2: pressure vessel body; 3: pressure vessel cap; 4: magnetic field coil; 5: holding nut; 6: insulating sleeve; 7: furnace; 8: O-ring seal; 9: zirconia powder insulation; 10: measurement cell.

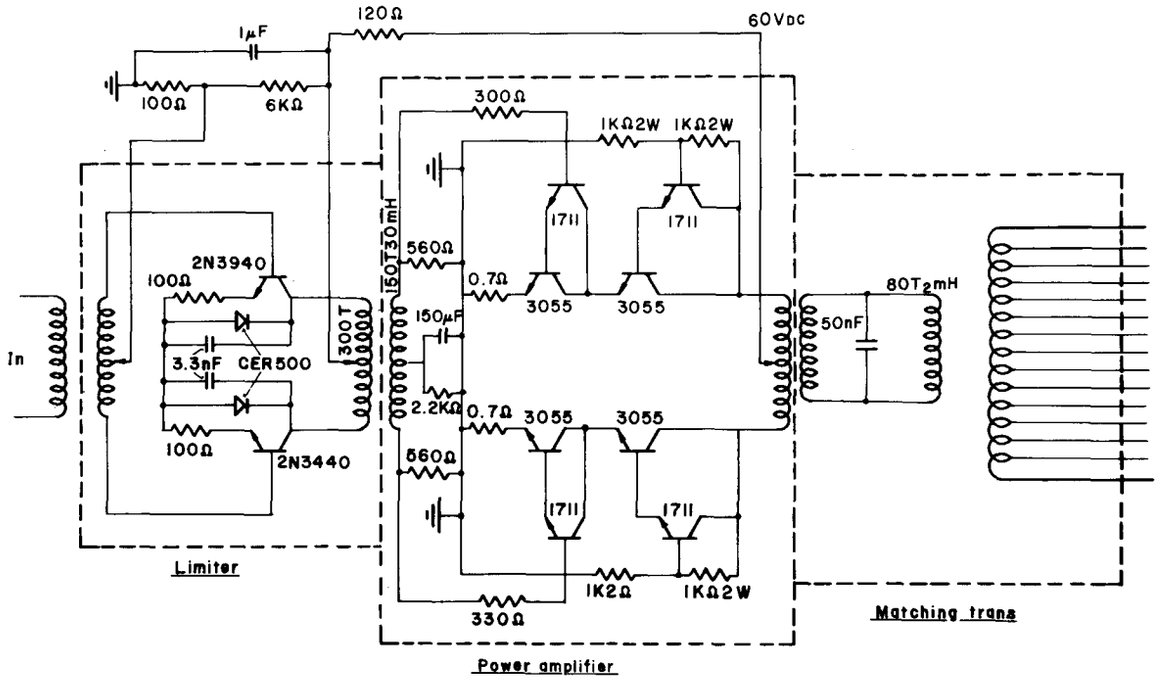

FIG. 3. Electronic scheme of Hall-current generator.

der was constructed from thin laminates of silicon steel packed closely together. The low intensity of the magnetic field, its relatively high frequency (1600 Hz), and its relatively high homogeneity (better than 0.5% over the sample volume) prohibited the onset of circulating magnetohydrodynamic currents in the sample. The magnetic Reynolds number[5] was smaller than 0.1. The coil was operated at resonance by a capacitor bank which was connected in parallel. The current for the magnet was generated by a 10-kW narrow-band power amplifier designed and built in our laboratory. The main characteristics of this amplifier are (a) low harmonic distortion (0.1% at rated power), achieved by a push-pull design, over power capacity and narrow banding; (b) very

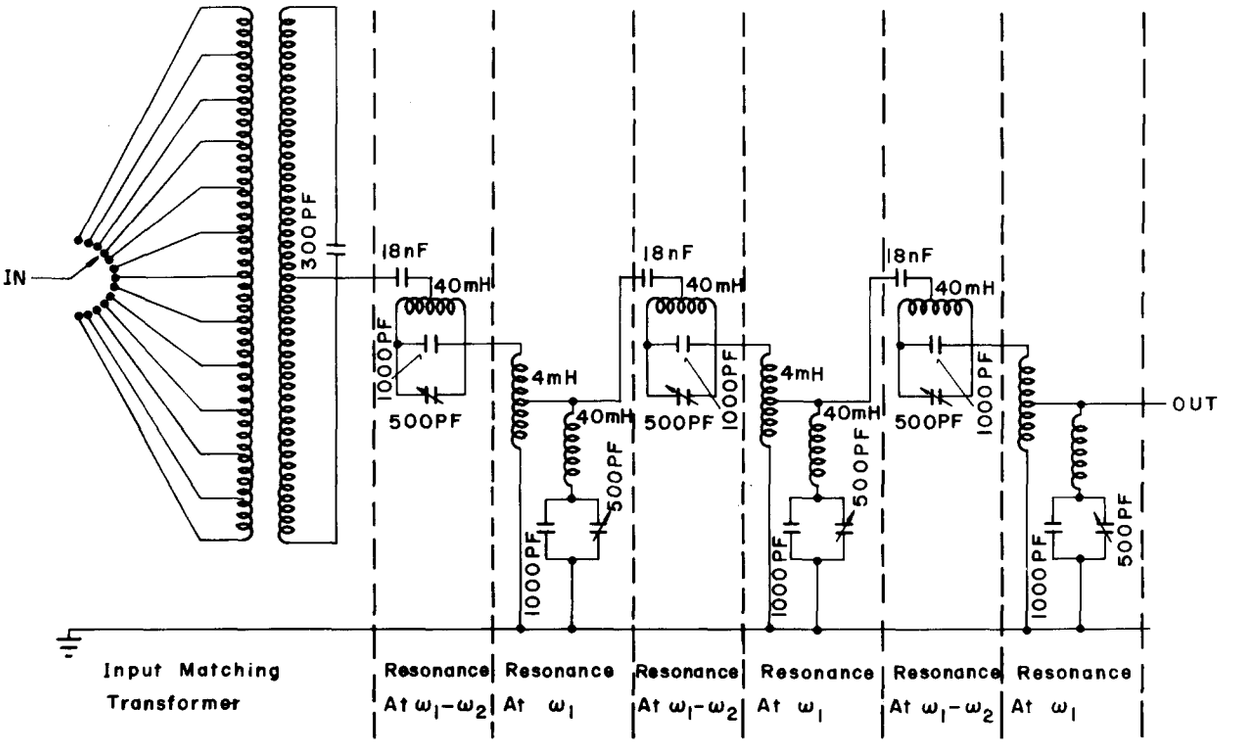

FIG. 4. Electronic scheme of first filter and input transformer.

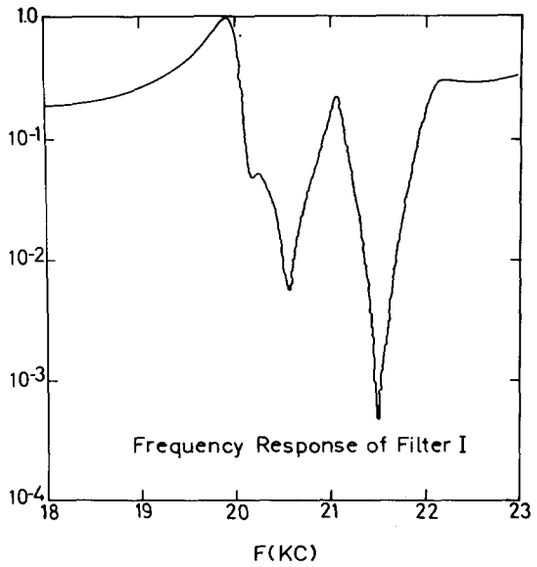

FIG. 5. Frequency response of the first filter. Note the efficient pass band at 20 kHz and the sharp notch at 21.6 kHz.

low residual FM intermodulation (less than 0.01%) to prevent mixing of two frequencies and thus generating a parasitic Hall signal; (c) low white noise (−140 dB).

V. HALL CURRENT

The Hall current was generated by a 10-W power amplifier designed and built in our laboratory (Fig. 3). This generator supplies a current (up to 5 A) at 21.6 kHz to the Hall sample, over an impedance range of 0.1–10 000 Ω (the metal-nonmetal transition). The essential points concerning the amplifier performance are the following: (a) very low residual intermodulation (less than 10^{-7}) to prevent modulation of the Hall current by pickups from the magnetic field; (b) low spurious noise (−120 dB). These requirements were achieved by amplifying the input signal to the saturation limit, generating a clean square wave (which cannot be amplitude modulated), which was subsequently passively filtered to reduce noise and harmonics. Output impedance is matched to the load by a tapped transformer.

VI. CHOICE OF FREQUENCIES

The double ac method[1,2] utilizes one frequency, w_1, for the Hall current and another frequency, w_2, for the magnetic field, while the Hall voltage is measured at the sideband frequencies $w_1 \pm w_2$. The upper limit for all frequencies is set by the skin effect in metallic mercury. We make use of the skin-effect equation[6]

$$\delta = 6.61(\rho/f\mathscr{H})^{1/2}, \tag{1}$$

where δ is the layer depth (mm), f the frequency (Hz), ρ the specific conductivity of the sample (relative to copper), and $\mathscr{H}$ the permeability of the sample (relative to copper. Utilizing the known mercury data and taking $\delta = 5$ mm (which is a factor of 10 higher than the sample depth to ensure homogeneous flow), one gets an upper limit of ~100 kHz for the relevant frequencies. Above this frequency currents are not distributed uniformly over the sample.

The lower-frequency limit is determined by the thermal time constant of the measurement cell. Elimination of the transverse thermomagnetic effect that appears on the Hall-voltage electrodes[2] is achieved by setting the Hall-voltage frequency above the characteristic thermal frequency. Estimating the thermal response time by[7]

$$T = cd^2/K, \tag{2}$$

where T is the thermal response time (sec), c the thermal capacity of the mercury sample (cal/cm^3), d the geometrical length characterizing transverse heat exchange in the sample (cm), and K the thermal conductivity of the mercury sample (cal/cm °C sec) one gets for mercury at room temperature and a 10-mm-wide cell $T \sim 0.1$ sec.

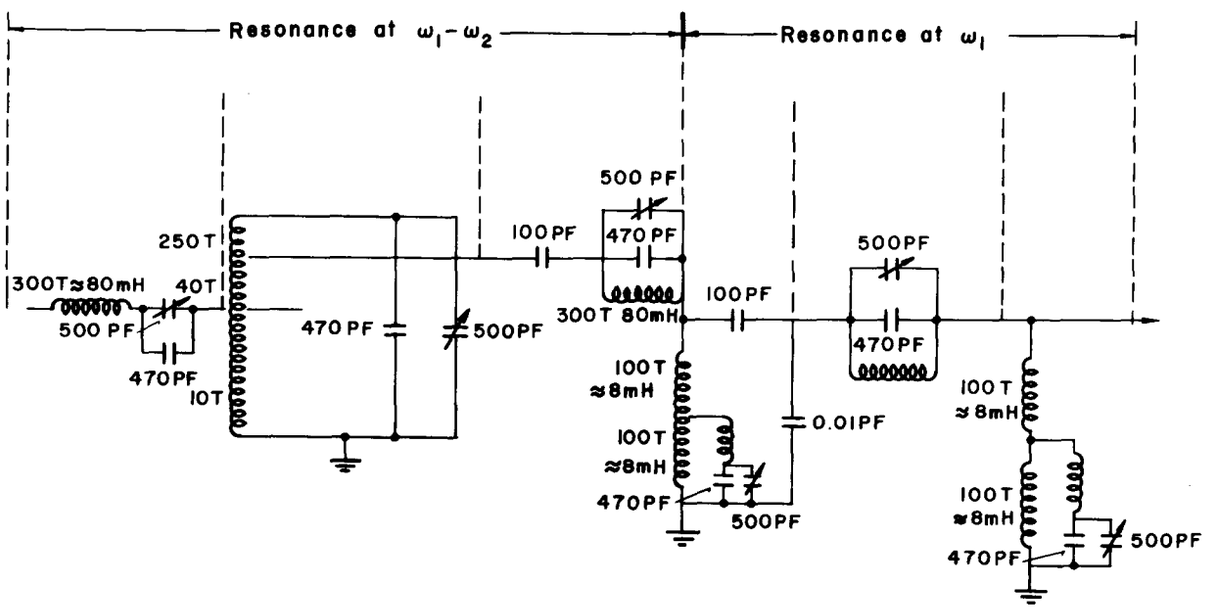

FIG. 6. Electronic scheme of the second filter.

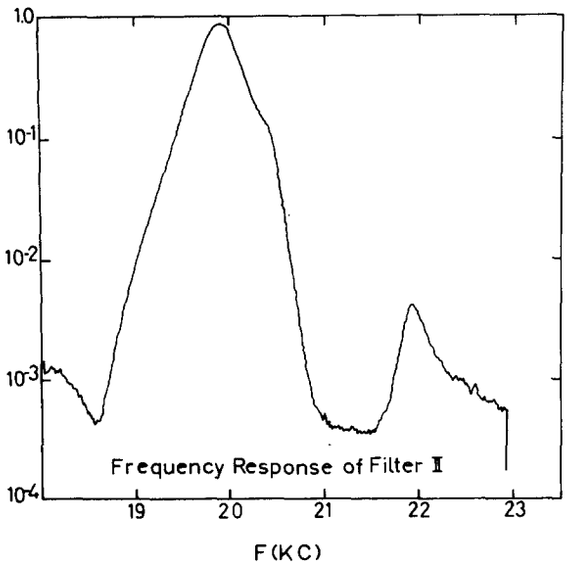

FIG. 7. Frequency response of the second filter. Note the broad resonance and notch.

Since the measured magnetothermal effect exhibits an exponential dependence on the thermal frequency ($f_T = T^{-1}$) in the form[8]

$$V_f = V_E \exp(-f/f_T), \tag{3}$$

where V_f = measured magnetothermal voltage, V_E = equilibrium magnetothermal voltage, f_T = thermal frequency, and f = measurement frequency, the measured thermal voltages will be sharply attenuated if we increase the transverse voltage frequency (at the low sideband, $w_1 - w_2$) above 100 Hz. The allowed frequency range covers most of the audio range (0.1—100 kHz).

The noise characteristics of commercial low-noise amplifiers (for example, P.A.R. amplifier 213 used by us) sets the optimum noise frequency at about 20 kHz. Since the power radiated by the magnetic field (3 kW) is much higher than that of the Hall current (3 W), and the radiated power increases with frequency, one usually selects the lower frequency for the magnet. These arguments led us to select the frequency $w_1 = 21\,600$ Hz for the Hall current, the frequency $w_2 = 1600$ Hz for the magnet, and the frequency $w_1 - w_2 = 20\,000$ Hz for the Hall voltage. The relatively high magnet frequency assures easy separation of the low sideband (20 000 Hz) from the carrier frequency (21 600 Hz) which simplifies the design of the filter stages.

VII. HALL-VOLTAGE DETECTION SYSTEM

In view of the limited intensity of the magnetic field and the high electron concentration in the metallic sample, the measured Hall voltages are very low (about 3×10^{-9} V at room temperature). The detection system constructed by us is capable of extracting this signal (with a signal-to-noise ratio of 30:1) in the presence of appreciably stronger interfering signals from the Hall current and from the magnetic field (which are about 120 dB stronger than the Hall signal at the Hall electrode). The general guidelines in the design of the detection system were as follows: (a) maintaining a good impedance match to extract maximum signal power; (b) extensive passive filtering to reduce pickups with their possible intermodulation distortion at the various amplification stages; (c) use of linear components to minimize intermodulation. Following the Hall signal path, the detection system can be divided into the following stages:

A. Impedance-match transformer and first filtering stage

Since this unit constitutes the first stage of the detection system, particular care has to be exerted in its design. All the coils in this unit are air cored to eliminate the inherent nonlinearities encountered in ferromagnetic core elements. Screening of various elements of this unit is crucial, as well as their proper placing. Screening is achieved by thick-wall aluminium plates. The tapped input matching transformer covers an input impedance range of 0.2—10 000 Ω, in 14 stages. The filter section consists of a cascade of three stages, each of them being of the resonance-notch type[9] (see Fig. 4). The resonance bandpass is tuned to the low sideband Hall-voltage frequency (20 Hz) and the notch reject band is tuned to the current frequency (21.6 kHz). The tuning was checked by a wave analyzer (Hewlett-Packard 302-A). The attenuation at the resonance bandpass is only 2 dB while attenuation at the reject band is better than 65 dB. The difficulties inherent in the design using an air-core inductor are apparent by the three maxima appearing in Fig. 5 (corresponding to each stage in the cascade instead of a single maximum). The noise figure for this transformer filter is less than 3 dB, while intermodulation between carrier frequency at 21.6 kHz and the magnet field frequency at 1.6 kHz is less than 0.001%.

B. Preamplifier and secondary filter

A low-noise preamplifier (P.A.R. 213) with a gain of 30 dB is used after the first filtering stage. This relatively low amplification assures that the preamplifier remains in its strictly linear region (better than 0.01%). The preamplifier is followed by a second filter (Fig. 6). The filter can be designed with ferrite inductors since most of the parasitic interferences (at w_1 and w_2) were atten-

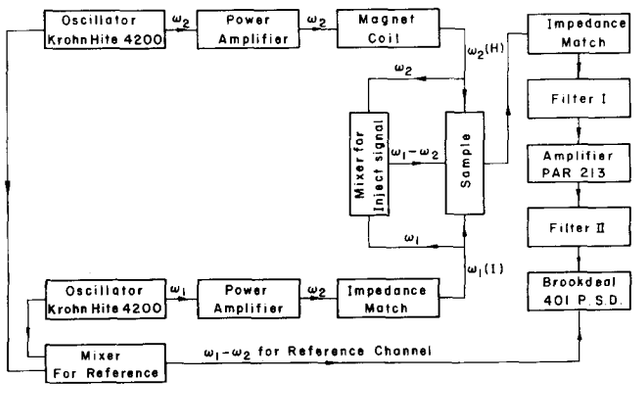

FIG. 8. Block diagram of electronic system for the Hall-voltage measurement.

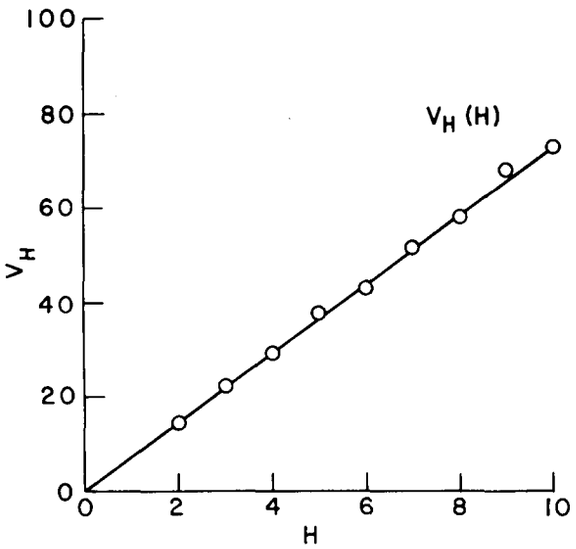

FIG. 9. Linearity check at constant current for liquid mercury at room temperature. $I_H = 4.1$ A/rms; $V_{H\max} = 4$ nV; $H_{\max} = 74$ G.

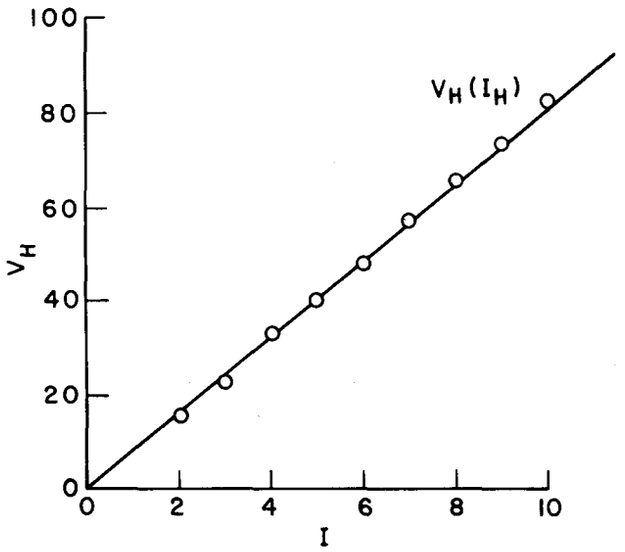

FIG. 10. Linearity check at constant magnetic field for liquid mercury at room temperature. $H = 74$ G; $V_{H\max} = 4$ nV; $I_{\max} = 4$A.

uated by the first filter. The main role of the second filter is to prevent intermodulation distortion and to prevent overloading of the lock-in amplifier used for the detection of the signal. This filter is also of the resonance-notch type, but is characterized by a considerably improved frequency response due to the ferrite inductors (Fig. 7). The efficient bandpass (attenuation less than 2 dB) and the efficient reject band (attenuation better than 65 dB) are relatively broad, so that frequent tuning is unnecessary.

C. Detection and calibration

Detection of the filtered signal is achieved by a phase-sensitive detector (Brookdeal, lock-in amplifier No. 401, England). The reference channel of the detector is fed from the two frequency generators (Krohn Hite 4200) which supply the Hall current and the magnetic field current, via a single sideband modulator. A calibration signal of controlled amplitude and phase was extracted from the Hall current and the magnetic field sources and injected into the measurement system in series with the Hall-voltage cell. The amplitude and the phase of this signal are chosen to obtain a null at the output of the phase-sensitive detector. This potentiometric measurement method reduces loading of the Hall voltage source and compensates for changes in over-all amplification or phase shifts. Since the calibration signal is generated (by a balanced modulator circuit) from the Hall current and from the magnetic field, it follows and compensates for their changes in time, thus avoiding frequent calibration checkups.

A block diagram of the electronic system is presented in Fig. 8. The operating performances of the detection system are (a) noise figure of 4 dB at 20 kHz (which is translated into noise voltage of 10^{-10} V at 10-sec integration time constant for mercury at room temperature); (b) parasitic signal less than 10^{-10} V; (c) accuracy of signal measurement 5%; (d) the Hall signal of mercury at room temperature is $\sim 3 \times 10^{-9}$ V.

VIII. ELECTRICAL CONDUCTIVITY MEASUREMENTS

The electrical conductivity is measured by the four-probes ac method. A current of 1—100 mA at 20 Hz was taken from a current source (built in our laboratory) and passed along the sample. The resulting voltage drop was measured by a lock-in amplifier (Brookdeal 401, England). This method allows resistance measurements over a wide range (10^{-5}—10^{4} Ω) at an accuracy of 2%.

IX. SYSTEM PERFORMANCE AND TYPICAL RESULTS

Linearity checks of the Hall voltage as a function of the magnetic field (at a constant current), and as a function of the Hall current (at a constant magnetic field) are

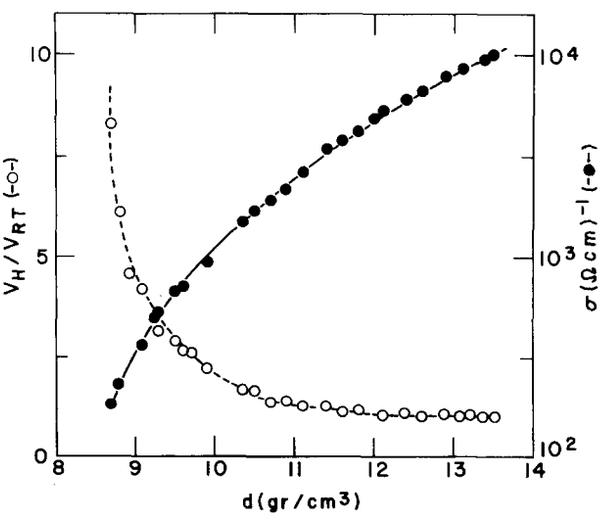

FIG. 11. Hall voltage (normalized to its room temperature value) and electrical conductivity of mercury as a function of density.

displayed in Figs. 9 and 10. The linear dependence yields strong support to the conclusion that most systematic errors in double ac systems have been eliminated. A comprehensive study[10] of spurious effects in the double ac method shows that sources of systematic errors which maintain the linear magnetic-field—Hall-current—Hall-voltage dependence are the following: (a) asymmetric Hall current; (b) asymmetric magnetic field; (c) current loop wires or voltage loop wires vibrate in the magnetic field; (d) sample vibrates in the magnetic field and periodic temperature changes modulate its resistance; (e) furnace vibrates in magnetic field inducing periodical temperature changes in the sample; (f) nonlinearity in the Hall-voltage detection. These sources of systematic errors have hopefully been avoided in our system by (i) choosing the Hall current, the magnetic field, and the Hall-voltage frequencies to be well above the mechanical or the thermal frequencies characterizing the sample; (ii) maintaining structural stiffness by using cements or crushed compressed powders to fill all voids and to decrease motional freedom; (iii) special attention was devoted to the linear performance of the critical parts in the detection system (i.e., sample contacts, first filter, and preamplifier).

Our measurements of Hall voltage in the temperature range 20—300 °C agree within the experimental uncertainty (±10%) with previously published results.[11,12] Typical experimental results for a mercury sample in the temperature range 30—1500 °C are displayed in Fig. 11. The Hall voltage is normalized to its room-temperature value (3.1×10^{-9} V). The density was calculated utilizing the recent equation-of-state data.[13] The physical interpretation of our results (Fig. 11) will be given elsewhere.[14]

[1]E. H. Putley, *The Hall Effect and Related Phenomena* (Butterworth, London, 1960).
[2]J. P. Jan, *Solid State Physics* (Academic, New York, 1957), Vol. 5, p. 1.
[3]F. Hensel and E. U. Franck, Rev. Mod. Phys. **40,** 697 (1968).
[4]I. K. Kikoin, A. P. Senchenkov, E. V. Gelman, M. M. Konsumskii, and U. S. P. Naurzakov, Sov. Phys.-JETP **22,** 89 (1966).
[5]W. B. Thompson, *An Introduction to Plasma Physics* (Pergamon, New York, 1962), p. 51.
[6]H. W. Sams, *Reference Data for Radio Engineers,* edited by H. P. Westman (Howard and Co., New York, 1969), Chap. 6.
[7]R. P. Tye, *Thermal Conductivity* (Academic, London, 1969), p. 149.
[8]J. C. Perron, Rev. Phys. Appl. **5,** 611 (1970).
[9]P. R. Geffe, *Modern Filter Design* (Illiff, London, 1964), Chap. 14.
[10]H. L. McKinsie and D. Tannhauser, J. Appl. Phys. **40,** 4954 (1969).
[11]A. J. Greenfield, Phys. Rev. A **135,** 1589 (1964).
[12]Y. Tieche, Helv. Phys. Acta **33,** 963 (1960).
[13]R. Schmutzler, Ph.D. thesis (University of Karlsruhe, Germany, 1971) (unpublished).
[14]U. Even and J. Jortner, Phys. Rev. Lett. **28,** 31 (1972).